Int. Symp. on Convective Heat and Mass Transfer in Sustainable Energy
April 26 – May 1, 2009, Tunisia

MODELING AND EXPERIMENTAL STUDIES FOR THERMAL PERFORMANCE OF A GROUND HEAT STORAGE SYSTEM INTEGRATED WITH A GREENHOUSE

Sami Kooli [1,*], Mariem Lazaar[1], Majdi Hazami[1], Abdelhamid Farhat[1] and Ali Belghith[2]
[1] Centre de Recherche et des Technologies de l'Energie
BP 95 Hammam-lif, Tunis, 2050 Tunisia
[2] Faculté des Sciences de Tunis
Département de Physique, Le Belvèdère 1002 Tunisia
([*] Corresponding author: samikooli2000@yahoo.fr)

ABSTRACT. A thermal model has been developed to investigate the potential of using the stored thermal energy of the ground for greenhouse heating and cooling with the help of a ground heat storage system (GHSS) integrated with the greenhouse located in the premises of CRTEn, Tunis, Tunisia. Experiments were conducted extensively throughout the years 2006-2007, and the developed model was validated against several consecutive arbitrary days experiments. The predicted and measured values of the greenhouse air temperatures and humidities that were verified, in terms of root mean square deviation and correlation coefficient, exhibited fair agreement. The results of this study showed that the GHS system kept the inside air temperature 1–3 °C higher than that of outside air at nighttime. The main reason for this low efficiency is due to the weak heat transfer area of the water-air heat exchanger. The simulation results indicate that the GHSS does not yield any significant effect for cooling greenhouses during sunny daytime. The GHSS fulfils its full potential for a heat transfer area of 150 m². With this area, there occurs 4–6 °C rise of temperature in greenhouse as compared to the temperatures without GHSS and respectively 5-7.5°C rise in greenhouse as compared to outside air.

NOMENCLATURE

D_T	soil moisture thermal diffusivity, $m^2/s.K$
dT	infinitesimal temperature difference, °C, K
D_θ	soil moisture diffusivity, m^2/s
e	thickness of tube, m
G_i	solar irradiance, W
H_i	thermal irradiance, W
J	radiosity, W/m^2
K_s	thermal diffusivity, m^2/s
l	caracteristic lenth of the leaf, m
L	latent heat of vaporisation of watr, J/kg
$\dot{m}$	water flow inside tube, kg/s
M	mass flux, kg/s
QC	sensible convective heat flux, W
QL	latent heat flux, W

QR net rate of heat loss by thermal radiation, W

QS absorbed solar radiation, W

Q_s soil heat flux, W

Q_u useful thermal energy, W

Q_v sensible heat flux due to ventilation, W

Ø diameter of tube, m

r_{ap} total crop resistance to water vapor diffusion, sm^{-1}.

r_{as} aerodynamic resistance of soil, sm^{-1}.

RE air infiltration rate, m^3/s

RH relative humidity, %

S source term, W/s

U wind velocity, m/s

U_c air velocity in the canopy, m/s

U_m mean air velocity inside the greenhouse, m/s

U_o overall Heat Transfer Coefficient, W/m^2K

V_a greenhouse volume, m^3

V_e root extraction term, 1/s

W specific humidity, kg/kg dry air

Greek letters

λ_s thermal conductivity of ground, W/m.K

σ Stefan-Boltzman constant

ρ reflectance

τ transmittance

θ soil volumetric moisture, m^3 water/m^3

δ spacing between capillary tubes, m

ρ_a density of air, kg/m^3

ΔT temperature difference

Subscripts

∞ sky

a interior air

c cover

oc outer cover face

ic inner cover face

i inlet, index

o external air, outside, outlet

h heat exchanger

int internal

ext external

m mean

j index

os surrounding ground

p plant, crop
s soil
s0 soil surface
s1 first soil layer
w water

Superscripts
* at saturation, solar

Abbreviation

EAHES Earth-air heat exchanger system

GHSS Ground heat storage system

WAHE Water-air heat exchanger

SWHE Soil-water heat exchanger

INTRODUCTION

In the Mediterranean regions, most of shelters are provided with hand-operated systems of ventilation and are not heated (or, in the best case, have some rudimentary heating system). The insufficient ventilation (during summer) and the lack of heating (during winter) lead to inappropriate extreme air temperature and humidity. Large diurnal amplitudes of air and soil temperatures are frequent, with too low temperatures during winter nights and too high temperatures during summer days. The consequence of these situations is that the resulting microclimate is far from being satisfactory for the crop during a large part of the year. The effects of this inadequate microclimate on the components of the production (yield, quality) are very negative.

These problems can be solved by some heat supply to the greenhouse during the winter critical periods and by forced ventilation or evaporative cooling during late spring and summer period. Unfortunately, the efficiency of cooling and heating systems based upon the use of fossil energy is affected by their very high investment and running costs. Consequently, it is necessary to use cooling and heating technologies such Water heat storage in ground tubes and barrels, North wall heat storage, earth-air heat exchanger systems (EAHES), rock bed storage, phase change material (PCM) storage, underground water heat storage and ground heat storage systems based upon the use of renewable energy which could be promising. Continuous research in this area and several successful demonstrations has resulted in rapid advancements and commercialization of these systems with satisfactory results. Based on the working principles, these systems have been classified into active and passive [Santamouris et al. 1994b].

Water heat storage in ground tubes and barrels was studied in several Mediterranean countries. Ground tubes were placed along the pathways between the plant rows. These water tubes covered usually 20–30% of the inside ground surface which could not be used for cultivation. Inside air temperature during winter nights was observed 2–4 °C higher as compared to outdoor conditions [Sethi and Sharma 2008]. Water tanks were placed vertically at the north side of greenhouses. The cost of these systems was low but the water containers occupied valuable ground space. In Roma (Italy) [Campoitti et al. 1988], in Dordogne (France) [Mercier 1982] and in Flagstaff (USA) [Santamouris et al. 1994b], the systems temperatures were observed to be 2–10°C higher than the minimum ambient air temperature.

The impact of north storage wall was studied on the inside air temperatures of several greenhouses PE covered. At Athens (37.90_N 23.70_E) Greece, at Chania Greece [Santamouris 1993] and at Quebec (46.80_N 71.38_W) Canada [Santamouris et al. 1994b], these systems satisfied about 35–50% heating needs of the greenhouses. In Gard Andure (France) [Banboul and Banbouserale 1987], the system was able to maintain 7–8 °C higher temperature inside the greenhouse as compared to outside conditions.

Few single systems, that can fulfill the required environmental conditions of the greenhouse by heating in winter and cooling in summer, are being used. The EAHES has gained an increasing acceptance during the last few years. EAHES have been studied in depth for creating a cooling effect inside greenhouses [e.g., Mihalakakaou et al. 1995, Gauthier et al. 1997]. The average greenhouse air temperature can be maintained 4–5 °C below ambient in summer. The earth temperature below its surface at a depth of about 3–4 m remains almost stagnant at about 26–28 °C throughout the year as studied by Santamouris et al. [1995]. Many studies conducted by researchers [e.g., Jaffrin et al. 1982, Kozai 1985, Immakulov 1986, Sawhney and Mahajan 1994, Sodha 1994] have presented the heating potential of EAHES. Underground pipes are buried at depths varying between 50 and 400 cm with spacing between them is 40 cm depending upon the size of the greenhouse. The heat exchangers are constructed using plastic, aluminum or concrete pipes, having 10–20 cm diameter. The greenhouse air temperature can be maintained 5–6 °C above ambient in winter. In Valencienne (50.21_N 03.32_E) France [Santamouris et al. 1996] and Athens (37.90_N 23.70_E) Greece [Mihalakakou et al. 994b], the systems were able to cover 62% heating needs of the greenhouse. However, the limitation of using the EAHES is the cost of digging the soil and laying the pipes up to 3–4 m depth. Horizontal layout of the pipe network at this depth is not easy. Moreover, for short term use, the temperature of the soil around the pipe mass gradually increases due to dissipation of heat from the outside pipe surface, thereby decreasing the efficiency of the system.

A popular and economical heat storage material is rock-bed (pebble, gravel and bricks).Various researches showed that the rock-bed system could achieve an inside air temperature 4–20 °C higher than the outside air, in combination with a variety of energy conservation methods [e.g., Bouhdjar et Boulbina 1990], and such systems could supply 20–70% of the annual heat requirement [Bredenbeck 1987]. Solar energy storage efficiencies of rock-bed systems varied from 8% to 19% [Willits et Peet 1987, Bouhdjar et al. 996, Ahmet et al. 2003].

Latent heat storage using phase change materials (PCMs) is one of the most efficient ways of storing thermal energy. A number of researchers during the past two decades have used organic compounds (paraffin waxes), hydrated salts and eutectic mixtures as PCMs for greenhouse applications. In an earlier study, it was reported that a phase change energy storage system using calcium chloride hexa-hydrate ($CaCl_2$ _ $6H_2O$ having melting temperature 29 °C and latent heat of fusion 191 kJ kg^{-1}) worked satisfactorily as a thermal storage unit [Kern and Aldrich 1979]. $CaCl_2$ _ $6H_2O$ (chliarolithe) was used to heat a 500 m^2 glasshouse situated at Nice (43.65_N 07.20_E) France in which roses were grown [Jaffrin et Cadier 1982]. Latent heat storage with 13.5 tons was placed in 9000 underground bags of 1.5 kg each. The arrangement provided 75% of the greenhouse heating needs with outdoor conditions 8.4 °C and 7.2 °C in December and January respectively (24 h average). In another study, a dehumidification process was added along with the CaCl2 _ 6H2O in a 500 m^2 glasshouse in which roses were grown [Jaffrin and Makhlouf 1987]. The greenhouse was situated in Nice (43.65_N 7.20_E) France. The system was able to cover 51% heating needs of the greenhouse in outside air conditions of 7–8 °C in December and January (24 h average). CaCl2 _ 6H2O was also used with extra water to heat an experimental greenhouse [McMullin and Ben-Abdallah 1988]. By adding extra water, melting point of the material was lowered by 3–4 °C and the heat of fusion increased. A quasi-eutectic mixture (serrolithe) was tested in 176 m^2 double skin polycarbonate cover greenhouse at Montfavet, France for lettuce-tomato rotation [Boulard et al. 1990]. A total of 2105 kg PCM was packed in 842 small containers (2.5 kg in each container) and placed along the north wall. Two 0.45 kW helicoidal fans were used to force the air through the storage. The greenhouse air temperature was maintained 7–8 °C higher as compared to outside air during nighttime.

Underground water heat storage consisted in a system which combines an underground water tank and air–water heat exchanger. This system was used to heat 500 m² PE covered greenhouse [Grafiadellis 1987] at Salonika (40.38_N 22.58_E) Greece. Water (60 m^3) was stored in tanks and vegetables were grown inside the greenhouse. The system was able to maintain inside room air temperature 5–6 °C higher than the outdoor conditions.

In this study, a Ground Heat Storage System (GHSS) which combines an underground soil-water heat exchanger (SWHE) and water-air heat exchanger (WAHE) is proposed. Like EAHES and rock-beds, GHSS uses the ground potential for thermal control of the greenhouse. The advantage of the proposed system over EAHES and rock-beds is that high humidity often observed in greenhouse with these systems [Willits et al. 1985], it is not with GHSS. This study is aimed to define the full potential of the GHS System. An experimental study has been performed to illustrate the overall system performance. A sophisticated model has also been developed to simulate the system performance with an aim to study the improvement in the effectiveness of the GHSS.

EXPERIMENTAL SET UP AND INSTRUMENTATION

The experiments were carried out in an east-west oriented 0.18 mm polyethylene tunnel greenhouse located in CRTEn (Tunisia) (latitude 36°43’ N, longitude 10°25’ E and altitude 3 m from mean sea level), with 8 x 12.5 m² effective floor covering area and 3.5 m central height. The greenhouse was integrated with the designed GHSS as shown in Figure 1.

The GHSS consisted of two (10 m long, 6 m wide) buried capillary plaits in polypropylene (Figure 1-a) (with thermal conductivity λ = 0.22 Wm/K) put respectively at 70 and 60 cm depth and connected to a water-air heat exchanger (Figure 1-b) through a circulating water pump. One meter width of a capillary plait was formed by 96 capillary pipes having 2 mm internal diameter, spaced to each other by 10 mm and connected to two 20 mm diameter collectors. This shape assured both a uniform temperature and heat flux in the soil around plait. The capillary plait has the advantage to be flexible, easily usable and with low costs and has the inconvenient to not resist to UV radiations. The water-air heat exchanger consisted of 42 ringed polyethylene tubes type ‘Agrotherm’ having 25 mm external diameter connected to two 60 mm diameter collectors. Agrotherm type tubes are generally used for greenhouse heating with geothermal source.

Experiments were conducted separately for four cases: greenhouse without any heating arrangement; greenhouse with GHSS, greenhouse with underground heating and greenhouse with inside air heating. For the soil and air heating, a heat pump type Clivet with nominal power 21.9 kW was connected separately to earth-water heat exchanger and to water-air heat exchanger providing water at controlled temperature. The range of water temperature delivered was between 30°C and 50°C, with the respectively flows 0.5 m3/h and 1.92 m3/h.

(a) (b)

Figure 1. the greenhouse integrated with the designed GHSS: (a) buried capillary plaits (b) Agrotherm tubes ringed inside the greenhouse

The quantities to be measured during an experimental run are soil temperature at various depths, soil surface heat flux, solar radiation inside and outside greenhouse and internal and external relative humidity and air temperatures. All soil temperatures were measured using (chromel–allumel) type K thermocouples. Eight thermocouples were installed at the following depths 0 cm, 10 cm, 20 cm, 30 cm, 40 cm, 50 cm, 60 cm and 70 cm. The thermocouple used to read the soil surface temperature (0 cm) was covered by a 1 mm thin soil layer to avoid errors due to direct solar radiation exposure. The thermocouples number was limited by the number of channels available in the AM416 Relay Multiplexer connected to a 21X CAMPBELL Scientific Data Acquisition System.

To measure soil heat flux a TCAV Averaging Soil Thermocouple Probe was used in conjunction with two HFT-3 Soil Heat Flux Plates. The TCAV is a temperature probe which parallels four thermocouple junctions (chromel–constantan) into one. The TCAV is constructed so two thermocouples can be used to obtain the average temperature of the soil layer above one heat flux plate and the other two above the second plate. The plates are buried at a fixed depth from the top of the soil of 8 cm to reduce errors due to vapor transport of heat. To measure solar radiation inside and outside the greenhouse two pyranometers LI-200SZ 5 model LiCor LI-200 which measures the total radiation falling on a horizontal surface were used. The precision of this sensor is approximately 5%. Measurement of internal and external relative humidity and air temperatures were made using a HMP35C Temperature/RH probe. The precision of this sensor, for the relative humidity, is about 3%. An SM192 Storage Module was used to provide a data transfer medium from the test site to the laboratory computer and to supplement the internal storage capacity of the 21X, allowing longer periods between visits to the site. Recordings were made at 10 min intervals during experiments by the 21X Campbell Scientific Data Acquisition System.

MODEL DESCRIPTION

The model considers a greenhouse divided into four layers, the air inside, the covering material, the crop and the soil beneath the greenhouse (see Figure 2). Figure 2 illustrates all of the fluxes of energy considered in the model. Single arrows represent individual fluxes and double arrows represent net radiative fluxes. These fluxes were listed in detail in Appendix.

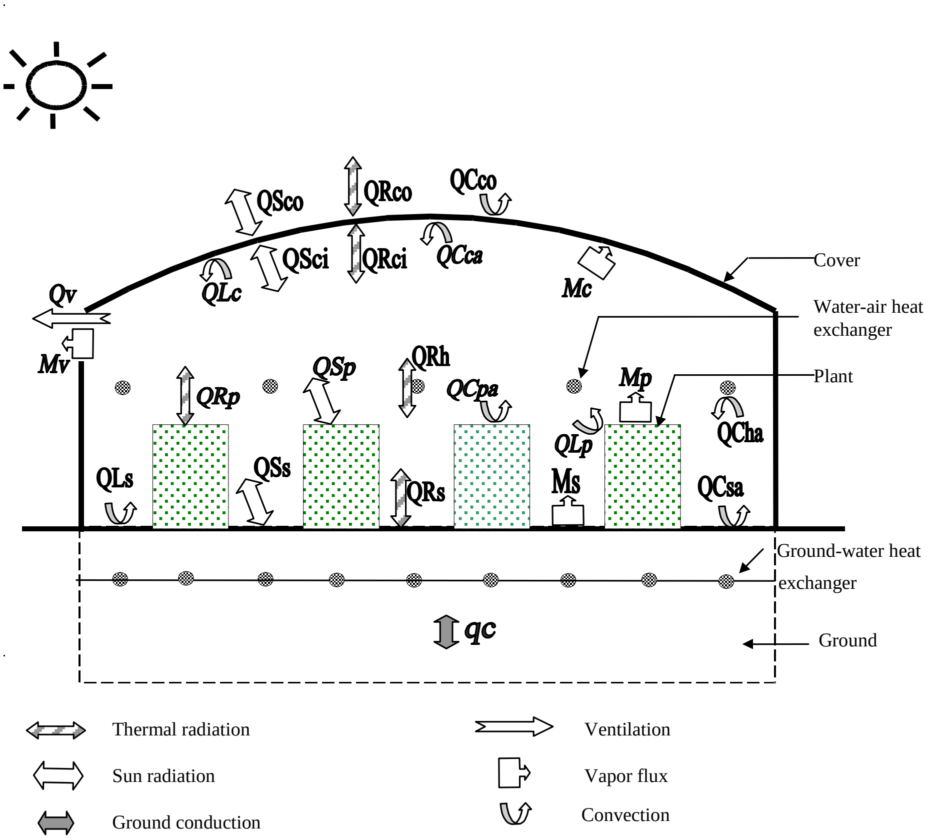

Figure 2. A schematic illustration of heat and mass fluxes existing in the greenhouse

Heat and mass balance equations are written for the air layer in order to predict its temperature and its moisture;
For air temperature:

$$\rho_a \, c_{pa} \, V_a \frac{dT_a}{dt} = -QC_{ac} - QC_{ap} - QC_{as} - QC_{ah} - Q_v \tag{1}$$

For air moisture:

$$\rho_a V_a \frac{dW_a}{dt} = -M_c + M_p + M_s - M_v \tag{2}$$

For covering material and crop, heat storage capacities are negligible in comparison to the diurnal energy fluxes and therefore steady state equations may be used. Two energy budget equations are written in order to predict cover and vegetation temperatures;
For cover temperature:

$$QR_{oc} + QR_{ic} + QS_{oc} + QS_{ic} + QC_{ca} + QC_{co} + LM_a = 0 \tag{3}$$

For vegetation temperature:

$$QR_p + QS_p + QC_{ap} - LM_p = 0 \tag{4}$$

In the soil layer, the two-dimensional heat diffusion equation is written:

$$\frac{\partial T_s}{\partial t} = K_s(\theta)\left(\frac{\partial^2 T_s}{\partial y^2} + \frac{\partial^2 T_s}{\partial z^2}\right) + \frac{S(y,z)}{C_s} \tag{5}$$

with the following boundary conditions:

- the soil surface temperature is computed from the soil air interface energy balance equation:

$$-\lambda_s A_s \left.\frac{\partial T_s}{\partial z}\right)_{z=0} = QC_{as} + QR_s + QS_s - LM_s \tag{6}$$

- at a certain prescribed depth an imposed temperature equal to a seasonal average ambient temperature.

Where T_s is the soil temperature, C_s is the volumetric soil heat capacity and $K_s(\theta)$ is the thermal diffusivity depending on soil moisture. The thermal diffusivity was calculated according to De Vries [1963] from the volume percentage of the soil components and the soil temperature. The source term S(y,z) is the infinitesimal rate of useful thermal energy from the earth to water heat exchanger. S(y,z) was calculated at each time step of the simulation using:

$$S(y,z) = \frac{\dot{m}\, c_{pw}\, dT_f(y)}{\delta} \tag{7}$$

where the outlet water temperature from the earth to water heat exchanger was calculated like for the water to air heat exchanger (Appendix) by replacing T_a by T_{sp}, the temperature of the ground in which the earth-water heat exchanger is installed, in Equation (A22) and using U_{oi} expressed as:

$$U_{oi} = \frac{1}{\dfrac{\phi_m}{h_{\text{int}}\phi_{\text{int}}} + \dfrac{e}{\lambda}} \tag{8}$$

Equations (1) and (2) represent a system of two first order differential equations. A fourth order Runge Kutta method was used for resolution. Equations (3, 4) and (6) represent a system of three non linear equations with four unknowns T_c, T_p, T_{s0} and T_{s1}. The Newton-Raphson iteration procedure was used for resolution. T_{s1} was determined by iteration on the total equations system. Equation (5) is parabolic. A volume finite approximation was used and the Peaceman and Rachford ADI schema was adopted for resolution [Ting-Yuan and Charlie 2003].

RESULTS AND DISCUSSION

In order to understand the outdoor climate effect on polyethylene tunnel greenhouse climate without any heating arrangement, the ambient and greenhouse conditions during the year 2006 are presented in Table 1. The greenhouse micro-climate was amplified with regard to outdoor. The monthly averages minimum air temperature inside and outside the greenhouse were almost the same indicating the needs of heating during the winter period (December to Mars). The monthly minimum values of daily minimum air temperature inside the greenhouse were always slightly greater than those of outside indicating the efficiency of the greenhouse during extremes air temperatures. The maximum values of daily minimum air temperature inside the greenhouse were often lower than those of outside indicating the inversion temperature phenomenon often observed in plastic tunnel greenhouses. The monthly averages maximum air temperature inside and outside the greenhouse indicates that it's not recommended to use shelters for cultivation during the summer period (June to September).

The monthly averages soil temperatures at a depth of 70 cm were varied from 16.2°C in January to 28.3°C in September. Theses deep soil temperature changes were dominated by the outdoor climate seasonal variation during the year. The soil and greenhouse air temperature values obtained indicates that the ground potential can be used for thermal control of the greenhouse. During the night time in winter (December to Mars) and even in cold nights in May greenhouse air temperature is lower than soil temperature; the ground potential can be used for heating the greenhouse. During sunny day time (Mars to May and October), greenhouse air temperature is higher than soil temperature; the ground potential can be used for cooling the greenhouse.

Table 1
Ambient and greenhouse conditions during the year 2006

	Ts(70cm	daily T_e min			daily T_a min			daily T_e max			daily T_a max		
Month	mean	mean	min	max	mean	min	max	mean	min	max	mean	min	max
J	16,2	8,2	3,8	14,5	8,4	5,2	12,8	23,6	18,3	30,4	29	24,3	33,3
F	18,3	7,5	3,6	12,5	*	*	*	23,7	18,4	29,2	*	*	*
M	19,5	10	5	14,1	9,9	6,9	13,7	28	19,7	35,5	37,2	35,4	39,6
A	21,5	13,6	6,3	20,7	15,2	7,5	19,4	29,6	23	35,9	36	26,2	46,7
M	23,2	12,5	7,9	14,7	14,4	11	16,4	26,1	20,2	29,9	34,2	26,5	39,4
J	25,8	18,5	11,6	20,7	18,8	12,9	20,7	34,3	29	38,4	38,2	33	42,3
J	27,3	20,5	17,1	25,7	21	17,2	24,8	38,7	35,8	40,8	43,4	42	45,1
A	27,1	21,6	17,4	23,6	21,9	17,6	24,5	37,7	32,8	39,3	40,8	37,8	43,9
S	28,3	21,1	18	23,7	21,3	18,4	23,4	37,2	32,6	43,4	41,9	34,6	44,6
O	24,9	16,1	10,5	21,6	16,6	11,3	21,2	33,6	26,9	39,5	34,2	28,4	38,1
N	*	*	*	*	*	*	*	*	*	*	*	*	*
D	18,3	10,3	4,3	16,8	10,4	5,5	15,6	24,1	17,6	31	27,5	17,4	33,9

Typical time variation of soil temperature at the depths 10, 20, 30, 40, 50, 60 and 70 cm for greenhouse without heating and greenhouse with underground heating are respectively shown in figures 3 and 4. The heat source temperature 48° C is also plotted in figure 4. The curves obtained have clearly demonstrated the expected daily temperature variation in the soil and the damping of this oscillation as depth increased. Damping increases too with the heat source temperature [Balghouthi et al. 2005] .The ground can be divided into a subsurface layer and a deep layer. In the subsurface layer temperature changes were dominated by diurnal changes and heat stored during the day is restored at night; whereas in the deep layer diurnal temperature changes remain practically non-affected and were often dominated by the variation with time constant significantly larger than one day. The thickness of the subsurface layer was about 50 cm.

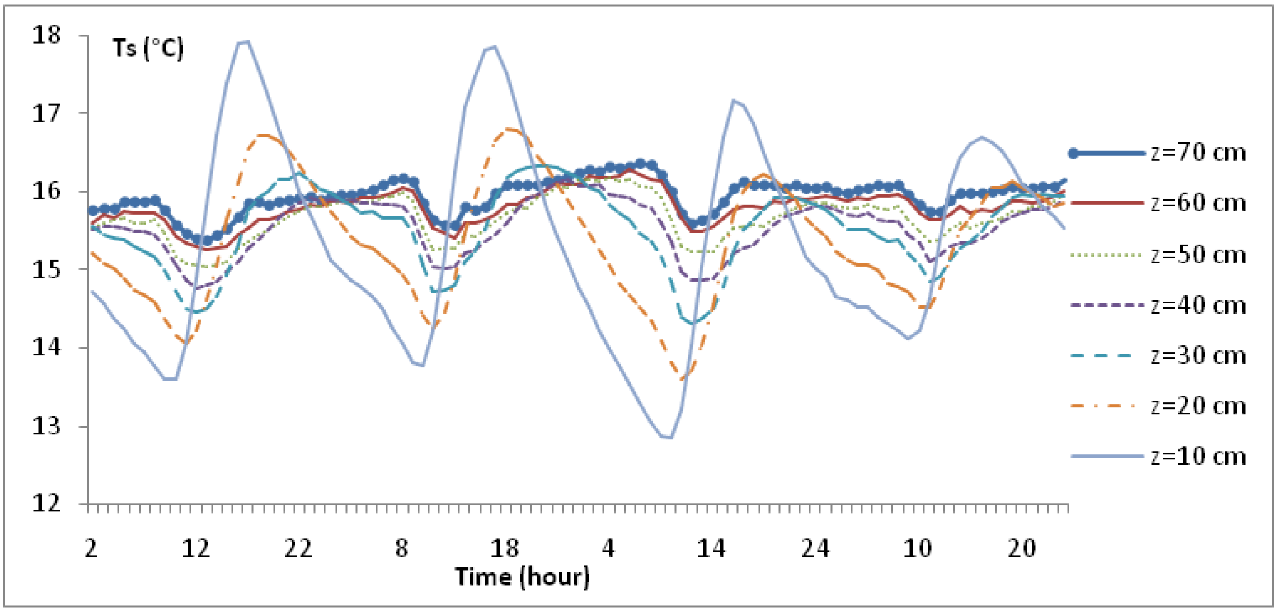

Figure 3. Variation of the soil temperature for various depths for greenhouse without heating

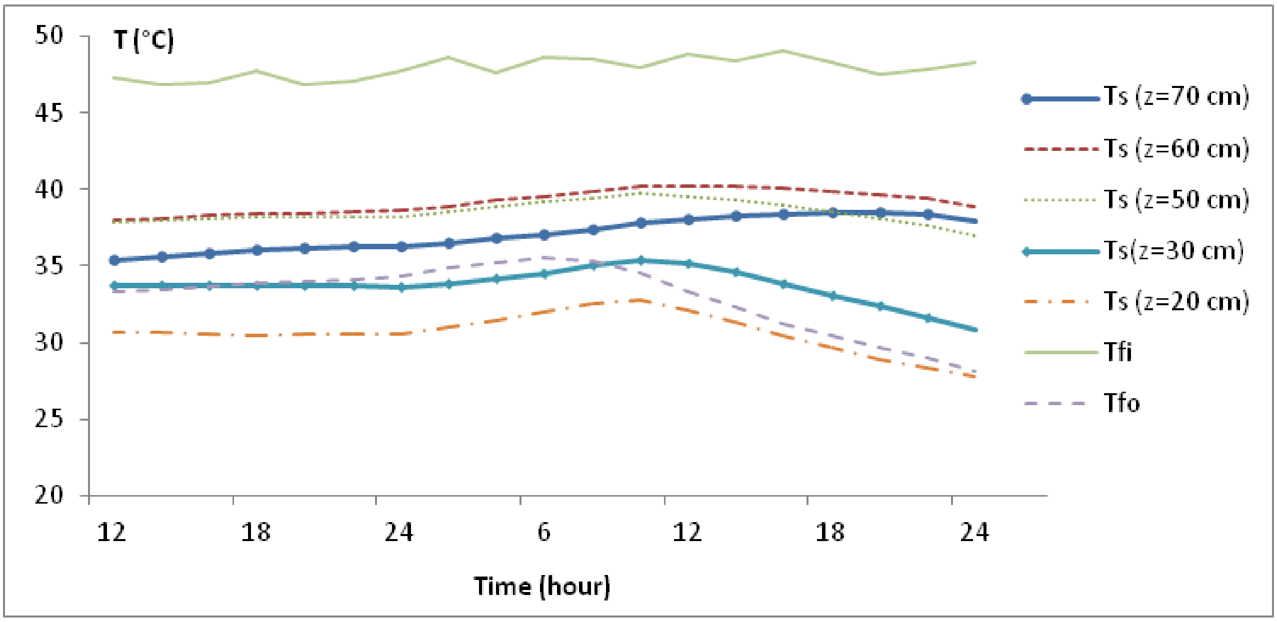

Figure 4. Variation of the soil temperature for various depths when the soil at 70 cm depth was heated at 48°C

In order to know the efficacy of the earth-to-water heat exchanger, typical time variation of heat exchanger inlet and outlet temperatures for the greenhouse with underground heating is shown in figure 5. Soil temperatures at depths 60 and 70 cm are also plotted in this figure. Soil temperatures at depths 60 and 70 cm and outlet water temperature were almost the same indicating the good efficiency of the earth-to-water heat exchanger. One should also notice 15°C difference between the outlet and inlet temperatures and the soil temperature neighboring the capillary plaits was maintained at approximately constant temperature indicating the high soil capacity for storing thermal energy. The above observations are confirmed by the useful thermal energy from the earth-to-water heat exchanger calculated according to (A21) and presented in tables 2.

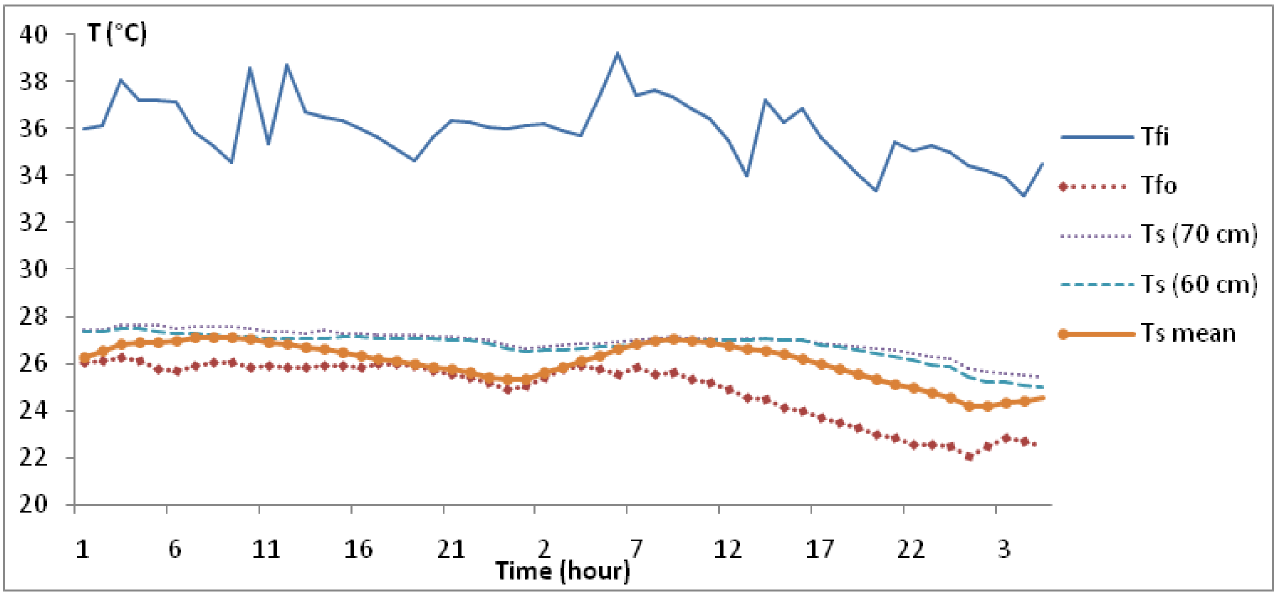

Figure 5. Variation of the soil temperature at 60 and 70 cm depths when the soil was heated at 36°C

Table 2
Thermal efficacy of the earth-water heat exchanger

T_{fi} °C	T_{fo} °C	T_s (70 cm) °C	T_s (60 cm) °C	T_{sm} °C	T_{sm}-T_{fo} °C	Q_u W
36,1	25,0	27,0	26,8	26,1	1,2	6441
31,1	25,1	27,7	28,1	26,4	1,2	3441
47,9	32,6	37,0	39,0	34,7	2,1	8851

In order to know the efficacy of the water-to-air heat exchanger, the useful thermal energy was calculated according to (A21) and presented in table 3. The outlet water temperature is far from inside air temperature and the difference between the outlet and inlet temperatures is weak (about 3°C) indicating the low efficiency of the water-to-air heat exchanger. The Agroterm tube is not adapted for low temperature use (less than 39°C) because of its weak heat transfer area (41 m²).

Table 3
Thermal efficacy of the water-air heat exchanger

T_{fi} (°C)	T_{fo} (°C)	T_a (°C)	Q_u (W)
48,8	45,7	31,3	6832
44,4	43,0	31,6	3074
39,7	39,1	33,9	1363

In order to know the efficacy of the GHSS, typical time variation of heat exchangers inlet and outlet temperatures, soil temperatures at depths 60 and 70 cm and air temperature inside and outside the greenhouse are shown in figure 6. The curves obtained have confirmed the above observations for the earth-to-water and for the water-to-air heat exchangers. Soil temperatures at depths 60 and 70 cm and outlet water temperature were almost the same indicating the good efficiency of the earth-to-water heat exchanger. The outlet water temperature is far from inside air temperature and the maximum mean differences between the outlet and inlet temperatures are weak (about 3.2°C during the day and -0.7°C during the night) indicating the low efficiency of the water-to-air heat exchanger and consequently that of the GHSS. Indeed, there occurs only 1–3 °C rise of temperature in night winter in greenhouse as compared to outside air.

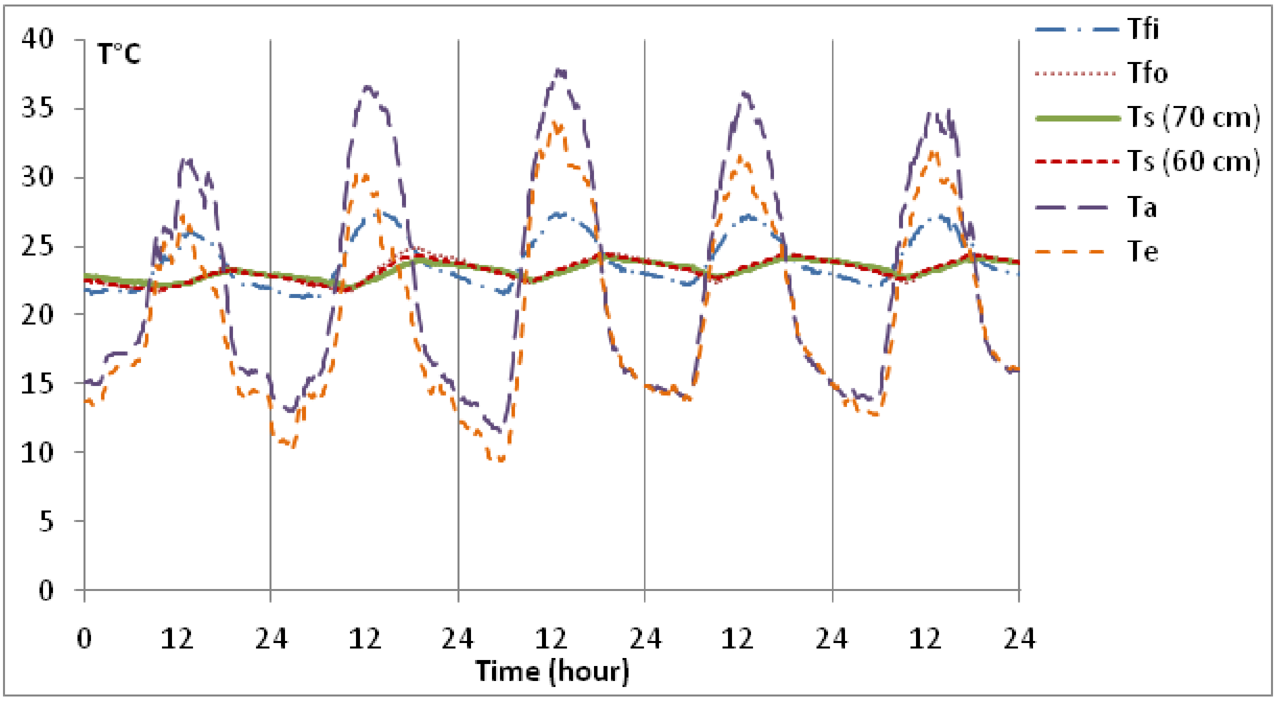

Figure 6. Typical time variation of heat exchangers inlet and outlet temperatures, soil temperatures at depths 60 and 70 cm and air temperature inside and outside the greenhouse

Figure 7 exhibits the evolution of surface heat flux and heat flux exchanged through the GHSS calculated according to (A21). During the day heat flux curves were under horizontal line of zero flux indicating that soil receives heat from greenhouse air. The received mean heat quantity throughout the GHSS was 336 Wh/m² (per day) about two times that received at soil surface (163 Wh/m²). During the night heat flux curves were above horizontal line of zero flux indicating that soil yields heat to greenhouse air. The yielded mean heat quantity through the GHSS was about 145 Wh/m² (per night) slightly more than the received heat quantity at soil surface (121 Wh/m²).

In order to validate the elaborated model, design and climatic parameter of experimental greenhouse without any heating arrangement have been used to compute greenhouse air temperature and humidity ratio. The results have been shown in Figures. 8 and 9, respectively. Experimental results have also been given in the same figures. The predicted and experimental temperature of air in the greenhouse showed fair agreement with coefficient of correlation (r') and root mean square of deviation (e') to be r' =0.89 and e'=1.1°C at nighttimes and 1.9 °C during daytimes, respectively.

Similarly, the predicted and experimental humidity ratio of air in the greenhouse showed fair agreement with coefficient of correlation and root mean square of deviation to be r'=0.94 and e'=2.8%, respectively.

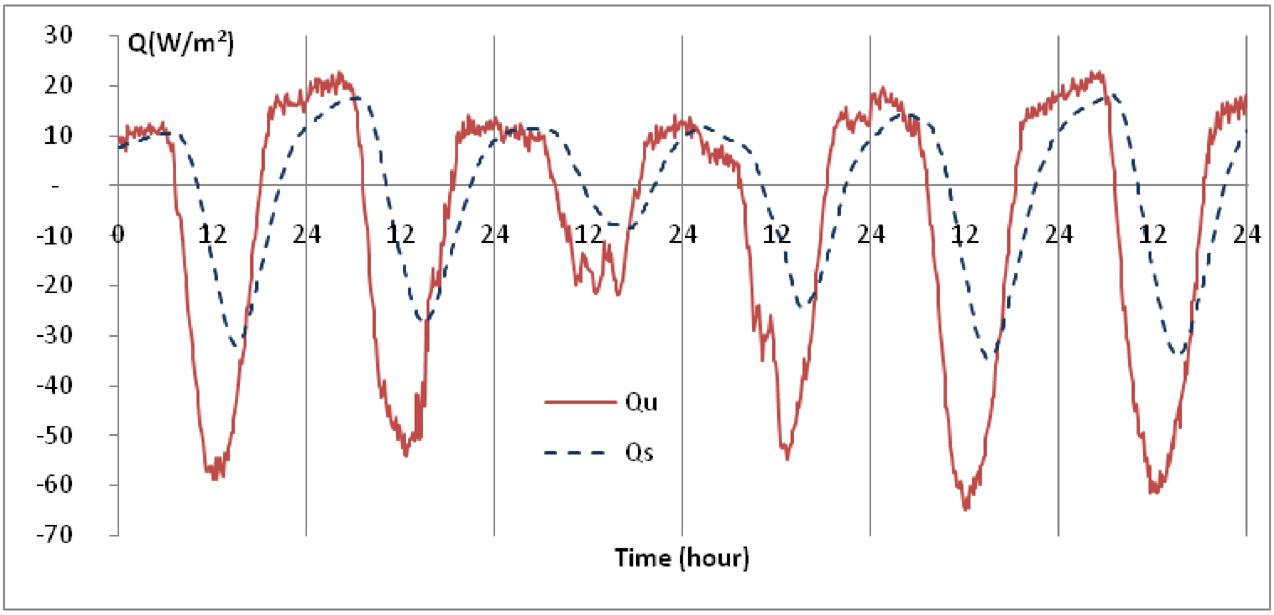

Figure 7. Evolution of surface heat flux and heat flux exchanged through the GHSS

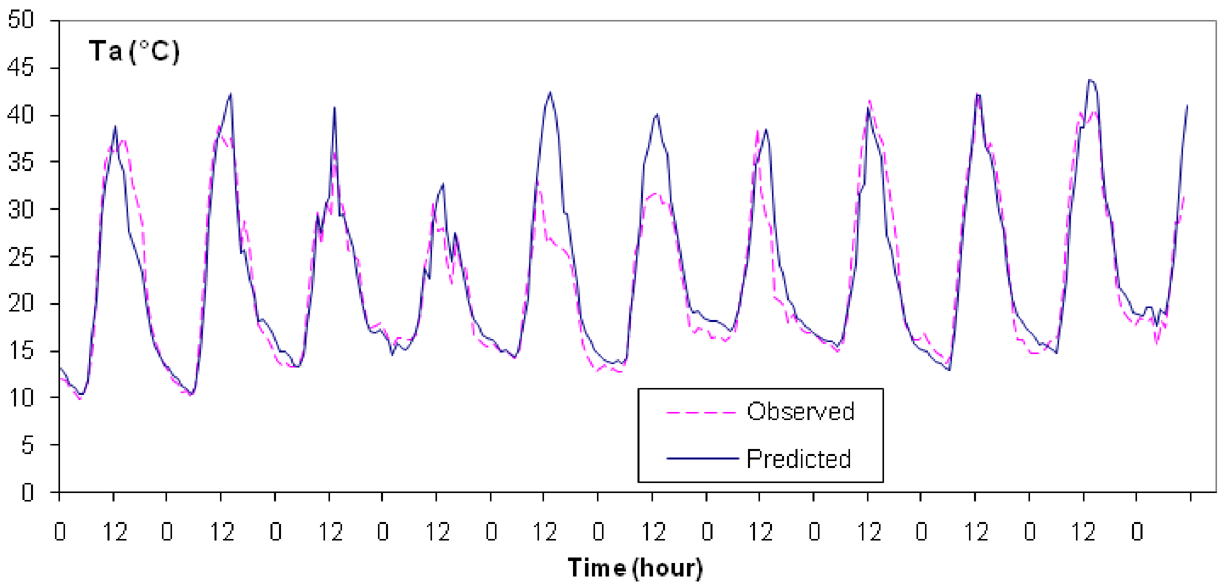

Figure 8. Predicted (dash line) and observed (full line) diurnal cycles of air temperature

The following curves show simulation results obtained for 10 days (from 11/09 to 21/09/2006) for a greenhouse with crops. Numerical simulation of water-air heat exchanger inlet and outlet temperatures, soil temperature at depth 70 cm and air temperature inside the greenhouse are shown in figure 10. The curves obtained have confirmed the above experimental observations. Soil temperature at depths 70 cm and outlet water temperature were almost the same indicating the good efficiency of the earth-to-water heat exchanger. The outlet water temperature is far from inside air temperature and the maximum mean differences between the outlet and inlet temperatures are weak (about 1.7°C during the day and -0.8°C at night) indicating the low efficiency of the water-air heat exchanger and consequently that of the GHSS.

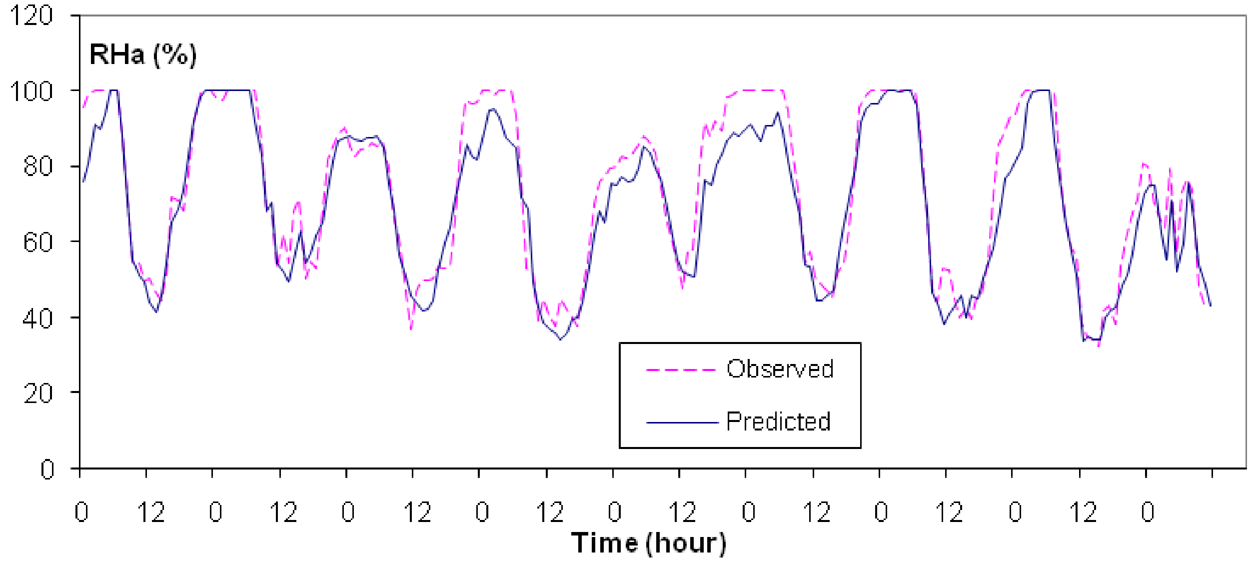

Figure 9. Predicted (dash line) and observed (full line) diurnal cycles of relative humidity

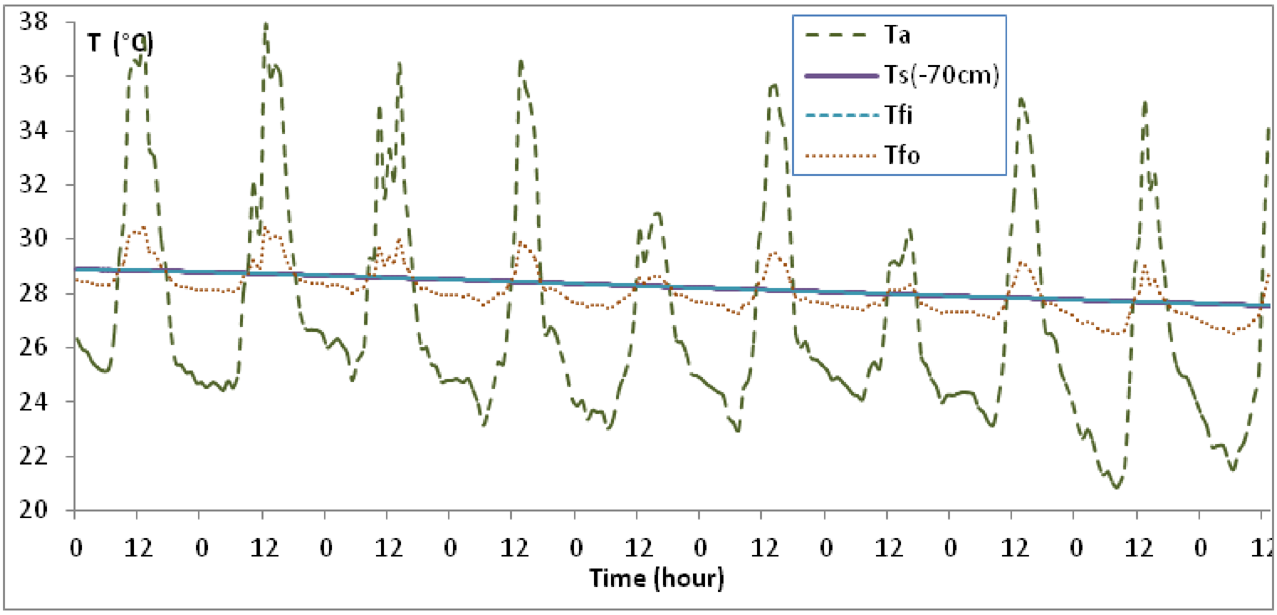

Figure 10. Predicted diurnal cycles of water-air heat exchanger inlet and outlet temperatures, soil temperature at depth 70 cm and air temperature inside the greenhouse

Figure 11 exhibit numerical evolution of inside air temperatures for greenhouses with and without GHSS. There occurs 1.9–2.5 °C and 0.5–1.6 °C rise of temperatures for the greenhouse air in the nighttimes and the daytimes, respectively, due to the incorporation of the GHSS as compared to the temperatures without the GHSS. Due to the high temperature of the ground (28°C) and thermal radiation emitted by the water-air heat exchanger, the GHSS contributes to heat the greenhouse even during daytimes.

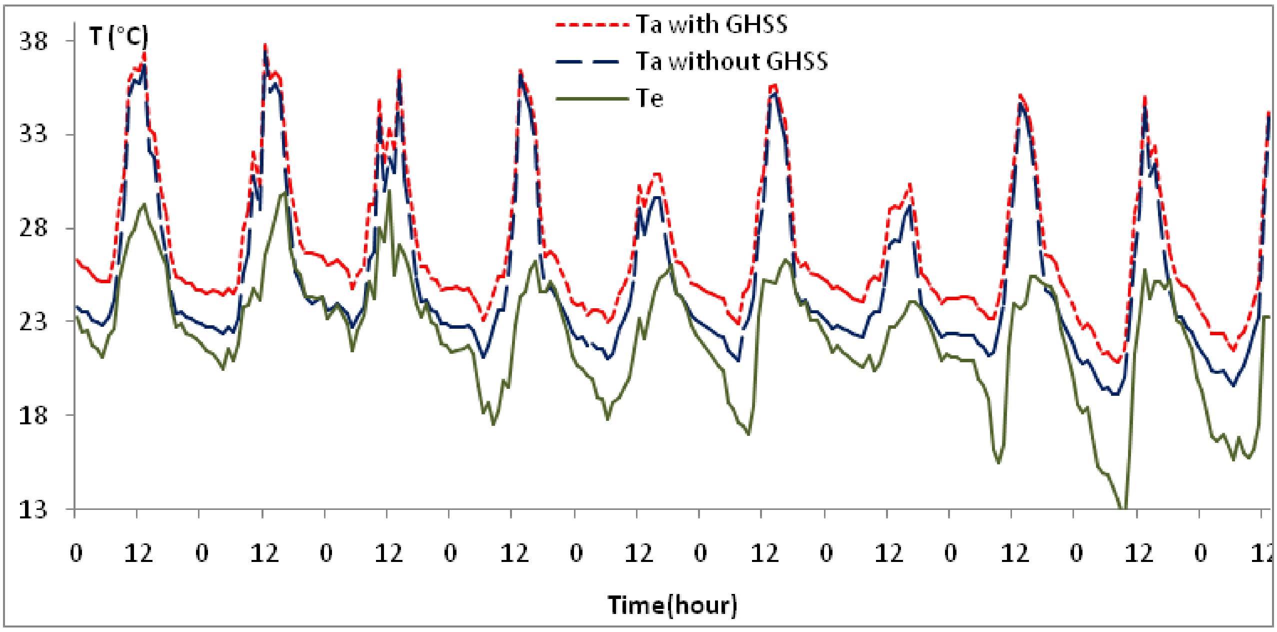

Figure 11. Predicted diurnal cycles of inside air temperatures for greenhouses with and without GHSS.

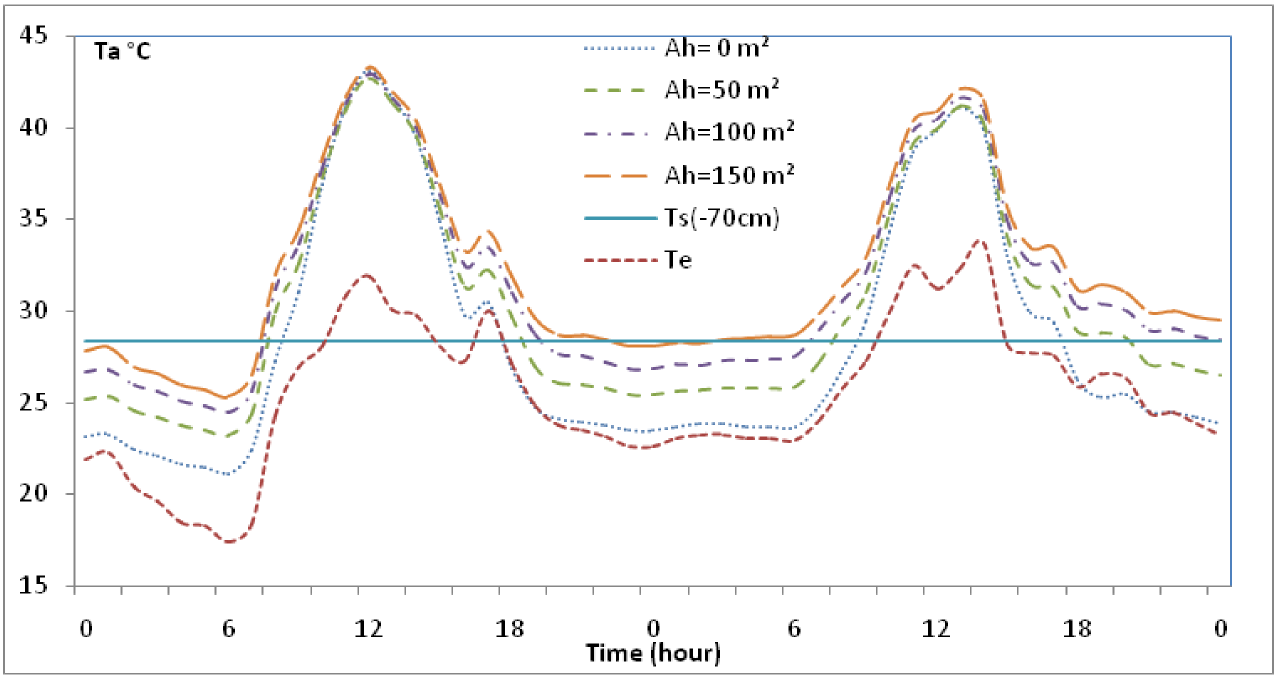

Figure 12. Effect of the heat transfer area of the WAHE of the greenhouse air temperature

The effects of the heat transfer area of the WAHE on the hourly variations of the greenhouse air temperature have been depicted in Figure 12. From the figure, it is seen that an increase in the heat transfer area causes an increase of the greenhouse air temperatures in the nighttimes. The GHSS fulfils its full potential for a heat transfer area of 150 m². There occurs 4–6 °C rise of temperature in greenhouse as compared to the temperatures without the GHSS and respectively 5-7.5°C rise in greenhouse as compared to outside air.

CONCLUSIONS

The main conclusions for the present study are as follows:
1. Use of the ground thermal potential for thermal control of greenhouses is viable in Tunisia. During night times in winter (December to Mars) greenhouse air temperature is lower than soil temperature; the ground potential can be used for heating greenhouses. During sunny daytime (Mars to May and October), greenhouse air temperature is higher than soil temperature; the ground potential can be used for cooling greenhouses.
2. There occurs 1–3 °C rise of temperature in night winter in greenhouse with GHSS as compared to outside air. The GHSS is not effective due to the low efficiency of the water to air heat exchanger since its weak heat transfer area.
3. The predicted and experimental temperatures and relative humidities of greenhouse air in the developed model exhibit fair agreement.
4. The results of simulation indicate that the GHSS does not yield any significant effect for cooling greenhouses during sunny daytime. The GHSS fulfils its full potential for a heat transfer area of 150 m². With this area, there occurs 4–6 °C rise of temperature in greenhouse as compared to the temperatures without the GHSS and respectively 5-7.5°C rise in greenhouse as compared to outside air.

APPENDIX

Convective Heat and Mass Transfer The sensible heat transfer from the inside air to the inner cover face (QC_{ac}), inside air to floor (QC_{as}), plant canopy to inside air (QC_{pa}), and outside air to outer cover face (QC_{oc}) were calculated using functional equations of the form

$$\boldsymbol{QC} = \boldsymbol{h}\, A\, \Delta T \qquad \text{(A1)}$$

where h represents the heat transfer coefficient, A the heat transfer area, and ΔT the temperature difference. The convective heat transfer coefficients calculated from Seginer and Livne [1978] were as follows:

$$\boldsymbol{h_{ac}} = 1{,}52\left|\mathrm{T_a} - \mathrm{T_c}\right|^{1/3} + 5{,}2\left(\frac{\mathrm{U_m}}{\mathrm{L_s}}\right)^{1/2} \qquad \text{(A2)}$$

$$\boldsymbol{h_{as}} = 1{,}52\left|\mathrm{T_a} - \mathrm{T_s}\right|^{1/3} + 5{,}2\left(\frac{\mathrm{U_c}}{\mathrm{L_s}}\right)^{1/2} \qquad \text{(A3)}$$

The convective heat transfer coefficient calculated from Stanghellini [1987] was:

$$\boldsymbol{h_{ap}} = \frac{\boldsymbol{\rho_a c_{pa}}\left(\ell\left|\mathrm{T_p} - \boldsymbol{T_a}\right| + 207\boldsymbol{U_c^2}\right)^{0,25}}{1174\,\ell^{0,5}} \qquad \text{(A4)}$$

The wind-induced heat transfer coefficient calculated from Von Elsner [1982] was:

$$h_{ce} = 6\, U^{0,8}\, L_s^{-0,2} \tag{A5}$$

The rates of water vapor diffusion from plant canopy to the surrounding air, and from greenhouse floor to the inside air were obtained from Penman [1948] as

$$M_p = A_p \rho_a \left(\frac{W_p^* - W_a}{r_{ap}} \right) \tag{A6}$$

$$M_s = \frac{A_s\, \rho_a\, (W_s^* - W_a)}{r_{as}} \tag{A7}$$

Stanghellini and De Jong [1995] give suitable expressions for obtaining the plant resistance to water vapor diffusion. Expressions for calculating the saturation humidity ratio W_p and W_s were also obtained from Campbell [1977].
From Wilhelm [1976] the rate of the inside air to moisture loss by condensation was determined from

$$M_a = A_c\, \rho_a\, h_{ac}^m\, (W_a - W_c^*) \tag{A8}$$

$$h_{ac}^m = \frac{h_{ac}\, L_e^{0.67}}{\rho_a\, c_{pa}} \tag{A9}$$

Sensible Heat and Moisture Flow due to Ventilation The amount of sensible heat associated with passive or forced ventilation is given by

$$Q_v = \rho_a\, RE\;\; c_{pa}\, (T_a - T_e) \tag{A10}$$

For passive ventilation the air infiltration rate RE, was calculated from Grimsrud and Sherman [1980] correlation equation

$$RE = A_{infltr} \sqrt{f_{wind}^2\, U^2 + f_{\Delta T}^2\, \Delta T} \tag{A11}$$

where f_{wind} and $f_{\Delta T}$ are empirical constants determined from Farhat et al. [2004].
The rate of moisture loss or gain due to passive or forced ventilation is given by

$$M_v = RE\, \rho_a (W_a - W_e) \tag{A12}$$

Thermal Radiation Exchange In calculating the thermal radiation exchange for the greenhouse components and the surrounding it was assumed that the greenhouse surfaces and the surrounding are grey, the surrounding sky is at an equivalent sky temperature, air inside the greenhouse does not participate in the thermal radiation exchange, and the greenhouse is taken as an enclosure with isothermal surfaces.
As recommended by Swinbank [1963] the equivalent sky temperature T_∞ was calculated from the outside temperature from the relation:

$$\boldsymbol{T}_{\infty} = 0{,}0552\, \mathrm{T}_{e}^{1,5} \tag{A13}$$

For a greenhouse enclosure having N isothermal opaque gray surfaces the net rate of heat loss by thermal radiation QR_i, for a typical surface I, having an area A_i, and surface emittance ε_i is the difference between emitted and absorbed radiative heat flux such as

$$\boldsymbol{QR_i} = \mathrm{A}_i\, \boldsymbol{\varepsilon}_i\, (\boldsymbol{\sigma}\mathrm{T}_i^4 - \mathrm{H}_i) \tag{A14}$$

$$\mathrm{H}_i = \sum_{j=1}^{N} \boldsymbol{J_j F}_{ij} \tag{A15}$$

$$\boldsymbol{J}_{i1} = \boldsymbol{\varepsilon}_{i1}\, \boldsymbol{\sigma}\, \mathrm{T}_i^4 + \boldsymbol{\rho}_{i1}\, \mathrm{H}_{i1} + \boldsymbol{\tau_i}\, \mathrm{H}_{i2} \tag{A16}$$

Equations (A14), (A15) and (A16) describe the radiosity for the most general case (non opaque surface) where H_{i1} and H_{i2} denotes irradiances of semi-transparent wall faces. These equations can be written in matrix form as

$$\begin{bmatrix} 1 & -(1-\varepsilon_s)F_{s-c} & 0 & -(1-\varepsilon_s)F_{s-p} & -(1-\varepsilon_s)F_{s-h} \\ -\rho_{ic}F_{c-s} & 1-\rho_{ic}F_{c-c} & 0 & -\rho_{ic}F_{c-p} & -\rho_{ic}F_{c-h} \\ -\tau_c F_{c-s} & -\tau_c F_{c-c} & 1 & -\tau_c F_{c-p} & -\tau_c F_{c-h} \\ -(1-\varepsilon_p)F_{p-s} & -(1-\varepsilon_p)F_{p-c} & 0 & 1-(1-\varepsilon_p)F_{p-p} & -(1-\varepsilon_p)F_{p-h} \\ -(1-\varepsilon_h)F_{h-s} & -(1-\varepsilon_h)F_{h-c} & 0 & -(1-\varepsilon_h)F_{h-p} & 1 \end{bmatrix} \begin{bmatrix} J_s \\ J_{ic} \\ J_{oc} \\ J_p \\ J_h \end{bmatrix} = \begin{bmatrix} \varepsilon_s \sigma T_s^4 \\ \varepsilon_{ic}\sigma T_c^4 + \tau_c J_o \\ \varepsilon_{oc}\sigma T_c^4 + \rho_{oc} J_o \\ \varepsilon_p \sigma T_p^4 \\ \varepsilon_h \sigma T_h^4 \end{bmatrix}$$

where J_e is the total flux of radiative energy away from the outside. For an insulated greenhouse Je is given from Kindelan [1980].

$$\boldsymbol{J_e} = F_{c\text{-}\infty}\, \boldsymbol{\sigma}\, T_{\infty y}^4 + F_{c\text{-}os}\, \boldsymbol{\varepsilon_s \sigma} T_o^4 \tag{A17}$$

where $F_{c\text{-}\infty}$ and $F_{c\text{-}os}$ are determined from
This system was solved using a matrix inversion procedure and then radiosities and net rate radiative heat fluxes were calculated.

Solar Radiation Exchange Solar radiation represents the main energy input to the greenhouse and therefore it should be carefully calculated. Assuming that solar radiation inside the greenhouse is scattered, in the present model an approach paralleling that used for thermal radiation exchange was adopted.
For a greenhouse enclosure having N surfaces the absorbed solar radiation QS_i, for a typical surface I, having an area A_i, and surface absorbtance α_i is written as

$$\boldsymbol{QS_i} = \boldsymbol{\alpha_i^*}\, \mathrm{A_i G_i} \tag{A18}$$

$$G_i = \sum_{j=1}^{N} \boldsymbol{J_i^* F}_{ij} \tag{A19}$$

$$\boldsymbol{J}_{i1}^* = \boldsymbol{\rho}_{i1}^*\, \mathrm{G}_{i1} + \boldsymbol{\tau_i^*}\, \mathrm{G}_{i2} \tag{A20}$$

Equations (A18), (A19) and (A20) describe the solar radiosity for face 1 of a semi-transparent wall. G_{i1} and G_{i2} denote irradiances of the two faces. These equations can be written in matrix form as

$$\begin{bmatrix} 1 & -\rho_s^* F_{s-c} & 0 & -\rho_s^* F_{s-p} \\ -\rho_{ic}^* F_{c-s} & 1-\rho_{ic}^* F_{c-c} & 0 & -\rho_{ic}^* F_{c-p} \\ -\tau_c^* F_{c-s} & -\tau_c^* F_{c-c} & 1 & -\tau_c^* F_{c-p} \\ -\rho_p^* F_{p-s} & -\rho_p^* F_{p-c} & 0 & 1-\rho_p^* F_{p-p} \end{bmatrix} \begin{bmatrix} J_s^* \\ J_{ic}^* \\ J_{oc}^* \\ J_p^* \end{bmatrix} = \begin{bmatrix} 0 \\ \tau_c^* G_{oc} \\ \rho_{oc}^* G_{oc} \\ 0 \end{bmatrix}$$

where G_{oc} is the amount of solar radiations reaching the outer face of the tunnel greenhouse cover obtained from Arinze et al. [1984].

Useful Thermal Energy from WAHE The useful thermal energy from the water to air heat exchanger is written as

$$\dot{Q}_u = \dot{m}\ c_{pw}\ (T_{fo} - T_{fi}) \tag{A21}$$

This flux includes the sensible heat transfer by convection from the water-air heat exchanger to the inside air (QC_{ha}) and the net rate of heat loss by thermal radiation from the water-air heat exchanger QR_h.

Where the outlet water temperature was calculated as follows:

Let the infinitesimal element of Agrotherm tube be dx in the direction of fluid (water) flow as shown in Fig. 1(b). The energy balance in the elemental section becomes

$$\dot{m}\ c_{pw}\ (T_{f,i+1} - T_{f,i}) = U_{o\ i+1/2} \left[T_m - \left(\frac{T_{f,i+1} + T_{f,i}}{2} \right) \right] \pi\phi_m \Delta x \quad \text{with} \quad 0 \le i \le N-1 \tag{A22}$$

Rearranging Eq. (22), the inside fluid temperature equation becomes

$$T_{f,i+1} = A\, T_{f,i} + B \qquad \text{with} \quad 0 \le i \le N-1 \tag{A23}$$

Where $$A = \frac{1 - \dfrac{U_{o\ i+1/2}}{2\dot{m}\ c_{pw}} \pi\phi_m \Delta x}{1 + \dfrac{U_{o\ i+1/2}}{2\dot{m}\ c_{pw}} \pi\phi_m \Delta x} \quad \text{and} \quad B = \frac{\dfrac{U_{o\ i+1/2}\ T_m\ \pi\phi_m \Delta x}{\dot{m}\ c_{pw}}}{1 + \dfrac{U_{o\ i+1/2}}{2\dot{m}\ c_{pw}} \pi\phi_m \Delta x} \tag{A24}$$

$$U_{oi} = \frac{1}{\dfrac{\phi_m}{h_{\text{int}}\phi_{\text{int}}} + \dfrac{e}{\lambda} + \dfrac{\phi_m}{h_{ext}\phi_{ext}}} \tag{A25}$$

h_{int} and h_{ext} were determined from using nusselt number according to Churchill and Chu [1975].

REFERENCES

Ahmet, K. Sefai, B. and Burhan, O. [2003], A study on the solar energy storing rock-bed to heat a polyethylene tunnel type greenhouse, Renewable Energy, Vol. 28, pp. 683–697.

Arinze, E. A. Schoenau, G. J. and Besant, R. W. [1984], A dynamic thermal performance simulation model for an energy conservation greenhouse with thermal storage, Transaction of ASAE, Vol. 27, pp. 508-519.

Balghouthi, M. Kooli, S. Farhat, A. Daghari, H. and Belghith, A. [2005], Experimental investigation of thermal and moisture behaviors of wet and dry soils with buried capillary heating system, Solar Energy, Vol. 79, pp. 669–681.

Banboul, T. and Banbouserale, J. [1987], Heating of greenhouse with solar energy, In: Bilgen, E., Hollands, K.G.T. (Eds.), Proceedings of ISES Solar World Congress, Hamburg, pp. 3350–3352.

Bouhdjar, A. Belhamel, M. Belkhiri, F. E. and Boulbina, A. [1996], Performance of sensible heat storage in a rockbed used in a tunnel greenhouse, In: Proc. World Renewable Energy Congress, pp. 724–728.

Bouhdjar, A. and Boulbina, A. [1990], In: Sayigh A, editor. Proc Congress Energy and the Environment, Reading, UK, pp.23–25.

Boulard, T. Razafinjohany, E. Baille, A. Jaffrin, A. and Fabre, B. [1990], Performance of a greenhouse heating system with a phase change material, Agricultural and Forest Meteorology Vol. 52, pp.303–318.

Bredenbeck, H. [1987], Energy saving greenhouse system with solar energy and rock bed storage, In: Von Zabeltitz C, editor. Greenhouse heating with solar energy, FAO, pp. 195–200.

Campbell, G. S. [1977], An introduction to environmental Biophysics, Springer-Verlay, New York, 155 p.

Campoitti, C. Camporcale, J. and Salice, R. [1988], Using geothermal energy as heat source for greenhouse heating, Acta Horticulturae, Vol. 246, pp. 556–558.

Churchill, S. W. and Chu, H. H. S. [1975], Correlating equations for laminar and turbulent free convection from horizontal cylinder, Int. J. Heat Mass Transfer, Vol. 18, pp. 1049-1053.

De Vries, D. A. [1963], Thermal properties of soils. In : W. R. Van Wijk (Editor), Physics of Plant Environment, North Holland, Amesterdam, pp. 210-235.

Farhat, A. Kooli, S. Kerkeni, Ch. Maalej, M. Fadhel, A.and Belghith, A. [2004], Validation of a pepper drying model in a polyethylene tunnel greenhouse, International Journal of Thermal Sciences, Vol. 43, pp. 53–58.

Gauthier, C. Lacroix, M. and Bernier, H. [1997], Numerical simulation of soil heat exchanger storage systems for greenhouses, Solar Energy, Vol. 60, No. 6, pp. 333–46.

Grafiadellis, M. [1987], Recent experiences with passive system for heating greenhouses. In: von Zabeltitz, C. (Ed.), Greenhouse Heating with Solar Energy, REU, Technical Series 1. FAO, ENEA, Roma, pp. 167–173.

Grimsrud, D.T. and Sherman, M.H., [1980], Infiltration-pressurization correlation: simplified physical modeling, ASHRAE Trans., Vol. 86, Part 2.

Immakulov, A. I. [1986], Storage of solar energy by forced circulations in shed greenhouses, Geliotechnika, pp. 22-44.

Jaffrin, A. Hallot, J. and Lubrano, M. [1982], Stockages thermiques et transferts par air humide dans les serres solaires, La Serre Solaire Architecture Agriculture, UNESCO.

Jaffrin, A.and Cadier, P. [1982], Latent heat storage applied to horticulture, Solar Energy, Vol. 28, No. 4, pp. 313–321.

Jaffrin, A. and Makhlouf, [1987], Use of solar energy for heating of greenhouses in mild winter climates, In: Bilgen, E., Hollands, K.G.T. (Eds.), Proceedings of ISES Solar World Congress, Hamburg, pp. 3358–3362.

Kern, M. and Aldrich, R. A. [1979], Phase change energy storage in a greenhouse solar heating system, ASAE, Paper No. 79-4028, Am. Soc. Agric. Engng., St. Joseph. MI.

Kindelan, M. [1980], Dynamic modeling of greenhouse environment, Transaction of ASAE, Vol. 23, No. 5, pp. 1232-1239.

Kozai, T. [1985], Thermal performance of a solar greenhouse with an underground heat storage system. In: Proceedings of the symposium on thermal applications of solar energy, Japan, ISES, p. 503.

McMullin, M. and Ben-Abdallah, N. [1988], An investigation of low temperature PCMs for short term energy storage in greenhouse, Canadian Agricultural Engineering, Vol. 30, pp.65–68.

Mercier, I. [1982], Design and operation of a solar passive greenhouse in south-west France, In: Proceedings of the International Congress on Energy Conservation and Fishculture, London, pp. 212–218.

Mihalakakaou, G. Santamourious, M. Asimakopoulos, D. and Tselepidaki, I. [1995], Parametric prediction of the buried pipes cooling potential for passive cooling applications, Solar Energy, Vol. 55, No. 3, pp. 163–73.

Mihalakakou, G. Santamouris, M. Asimakopoulos, D. and Papanikolaou, N. [1994b], Impact of ground cover on the efficiencies of earth-to-air heat exchangers, Applied Energy, Vol. 48, No. 1, pp. 19–32.

Penman, J. L. [1948], Natural evaporation from water soil and grass, Proc. Roy., Londre, Vol. 193, pp. 120-145.

Santamourious, M. Mihalakakou, G. Balaras, C. A. Agririou, A. Asimakopoulos, D. and Vallindras, M. [1995], Use of buried pipes for energy conservation in cooling of agricultural greenhouses, Solar Energy, Vol. 55, No. 2,pp. 111–24.

Santamouris, M. [1993], Active solar agricultural greenhouse: The state of art, International Journal of Solar Energy, Vol. 14, pp. 19–32.

Santamouris, M. Balaras, C. A. Dascalaki, E. and Vallindras, M. [1994b], Passive solar agricultural greenhouses: a worldwide classification and evaluation of technologies and systems used for heating purposes, Solar Energy, Vol. 53 No. 5, pp. 411–426.

Santamouris, M. Mihalakakou, G. Balaras, C. A. Lewis, J.O. Vallindras, M. and Argiriou, A. [1996], Energy conservation in greenhouses with buried pipes, Energy, Vol. 21, No. 5, pp. 353–360.

Sawhney, R. L. and Mahajan, U. [1994], Heating and cooling potential of an underground air-pipe system, Int. J. Energy Res., Vol. 18, pp. 509-524.

Seginer, I. and Levine, A. [1978], Effect of ceiling height on the power requirement of forced ventilation in greenhouse: a computational study, IBM Israel Scientific Center, Haifa, Israel.

Sethi, V. P. and Sharma, S. K. [2008], Survey and evaluation of heating technologies for worldwide agricultural greenhouse applications, Sol. Energy, Vol. 82, pp. 832–859.

Sodha, M. S. [1994], Thermal performance of parallel earth air-pipes system, Int. J. Energy Res., Vol. 18, pp. 437–47.

Stanghellini, C. and De Jong T. [1995], A model of humidity and its applications in a greenhouse, Agric. and Forest Meteor., Vol. 76, pp. 129-148.

Stanghellini, C. [1987], Transpiration of greenhouse crops, an aid to climate management, Ph.D. dissertation, Wageningen Agricultural University, Netherlands.

Swinbank, W.C. [1963], Long Wave radiation from clear skies, Quart. J. Roy. Meteo. Soc., Vol. 89, p. 339.

Ting-Yuan Wang, Charlie Chung-Ping Chen, [2003], Thermal-ADI—A Linear-Time Chip-Level Dynamic Thermal-Simulation Algorithm Based on Alternating-Direction-Implicit (ADI) Method, IEEE Transactions on very large scale integration (VLSI) systems, Vol. 11, No. 4, pp. 691-700.

Von Elsner, B. [1982], Das Kleinklima der Warmeverbrauch von geschlossenen Gewachshausern, Institut fur Technik in Gartenbau, Univ. Hannover, Heft, 12, 197 p.

Wilhelm L. R. [1976] Numeric calculation of psychrometric properties, Transaction of ASAE, Vol. 19, No. 2, pp. 318-325.

Willits, D. H. Chandra, P. and Peet M. M. [1985], Modelling solar energy storage systems for greenhouses, J. agric. Engng Res., Vol. 32, pp.73-93.

Willits, D. H. and Peet, M. M. [1987], Factors affecting the performance of rockstorages as solar energy collection/storage systems for greenhouses, Transactions of the ASAE; Vol. 30, No. 1, pp. 221–232.